American Mineralogist, Volume 77, pages 8–18, 1992

A ^{27}Al and ^{29}Si MAS NMR and infrared spectroscopic study of Al-Si ordering in natural and synthetic sapphirine

Andrew G. Christy
Department of Chemistry, University of Leicester, Leicester LE1 7RH, United Kingdom

Brian L. Phillips
Geology Department, University of Illinois, 245 Natural History Building, 1301 W. Green Street, Urbana, Illinois 61801, U.S.A.

Bernd K. Güttler
Physikalisch-Technische Bundesanstalt, Bundesallee 100, 3300 Braunschweig, Germany

R. James Kirkpatrick
Geology Department, University of Illinois, 245 Natural History Building, 1301 W. Green Street, Urbana, Illinois 61801, U.S.A.

Abstract

Magic-angle sample-spinning (MAS) ^{29}Si high-resolution NMR spectra are presented for a natural sapphirine sample from Aileron, Australia, synthetic sapphirine samples crystallized from a gel of $7MgO \cdot 9Al_2O_3 \cdot 3SiO_2$ composition and subjected to various heat treatments, and a more siliceous synthetic sample. A ^{27}Al NMR spectrum was also obtained from a synthetic sample.

The most intense peak in the ^{29}Si spectra is near -73.1 ppm for all samples. The synthetic samples also show distinct maxima near -75.5 and -78.0 ppm and a weak peak near -80.8 ppm. The similarity between the envelopes of these spectra and that of the natural sample suggests that the local Si environments are similar in all samples. The ^{27}Al spectrum showed only one maximum attributable to tetrahedral Al.

The ^{29}Si spectra are best fitted with a short-range ordering pattern in which one Q^3 site is almost completely occupied by Si and the other by Al. The location of the remaining Si is not well constrained. The Si concentration in one Q^3 site appears to maximize the number of Si-O-Al linkages in the tetrahedral chains.

Fourier transform infrared spectra over the wavenumber range 400–1300 cm^{-1} were obtained for one of the synthetic sapphirine samples and five natural sapphirine samples with different Si/Al ratios. All spectra were similar in general envelope. A progressive loss of resolution with increasing Si content suggests a concomitant increase in disorder in the natural samples. A heat-treated natural sample gave a spectrum that was badly resolved for its Si content. These data support the conclusions of the NMR study.

Introduction

Sapphirine is a characteristic mineral of Mg- and Al-rich, high-grade metamorphic rocks and is stable over a wide range of pressure, temperature, and bulk-rock composition (cf. Schreyer and Seifert, 1969; Hensen, 1987; Christy, 1988a). The chemical composition of sapphirine is approximately $[Mg_{4-x}Al_{4+x}]\,[Al_{4+x}Si_{2-x}]O_{20}$, with some substitution of Fe^{2+} for Mg and of Fe^{3+} for Al. Sapphirine occurs in several polytypic modifications (Merlino, 1973; Christy and Putnis, 1988). There is also considerable scope for cation order-disorder in the sapphirine structure. There are eight or nine octahedral sites and six tetrahedral sites in the average structures of the two most common polytypes (Moore, 1969; Higgins and Ribbe, 1979; Merlino, 1980). This paper is principally concerned with the state of Al-Si order on the tetrahedral sites and the effect of Al-Si order on the thermodynamic properties of sapphirine.

The thermodynamic properties of sapphirine are poorly known. Kiseleva (1976) attempted to derive enthalpies of formation and entropies for synthetic (Fe-free) and natural sapphirine. The synthetic material was calculated to be both more endothermic and higher in entropy, and this was ascribed to a difference in the state of cation order of the materials. This difference suggested that experimental studies on phase equilibria involving sapphirine might not be applicable to natural systems.

Unfortunately, it is difficult to determine the distribution of the various cations among the sites of the sapphirine structure. A major limitation is that all the cations occupy low-symmetry sites. Thus, change in the state of long-range order does not affect the crystal symmetry. Annealing experiments on natural sapphirine by Sahama

0003–004X/92/0102–0008$02.00

et al. (1974) showed small systematic changes in the cell parameters after heating, which may correlate with a change in the degree of cation order. However, quantitative determination of the long-range ordering pattern requires single-crystal refinement. Such refinements are not feasible for fine-grained synthetic samples such as those of the present study. Furthermore, the relatively long correlation length for diffraction techniques precludes the acquisition of short-range ordering data. This paper presents a study of Al-Si ordering in natural and synthetic sapphirine using nuclear magnetic resonance (NMR) and Fourier transform infrared (FTIR) spectroscopy.

NMR spectroscopy provides information on local atomic environments and has been used to investigate Al-Si ordering in a wide range of minerals, including clay phases, feldspars, and zeolites. The theory, experimental practice, and application of NMR spectroscopy in mineralogy have been reviewed by Kirkpatrick (1988) and Putnis (1988).

This paper presents high-resolution ^{27}Al and ^{29}Si magic-angle sample-spinning (MAS) NMR spectra of one natural sapphirine sample and a series of synthetic sapphirine samples. The spectra are interpreted in the light of likely Al-Si ordering schemes and related to heat-of-solution data.

One of the synthetic samples was also examined by FTIR spectroscopy, along with a series of natural sapphirine samples of different compositions. The mid-IR wavenumber range studied (400–1300 cm^{-1}) includes internal stretching and bending modes of the tetrahedra in the sapphirine structure (cf. Strens, 1974). The spectra obtained support the conclusions from the NMR spectroscopy and calorimetry regarding Al-Si ordering in sapphirine.

Previous work

Single-crystal refinements

There are three published single-crystal structure refinements for sapphirine: Moore's (1969) original X-ray structure determination for the *2M* polytype, a combined X-ray and neutron study of the *2M* phase by Higgins and Ribbe (1979), and a structure determination of the *1Tc* polytype by Merlino (1980). Table 1 lists the cation site occupancies from these three studies. Fe^{3+} has been included with Al in Table 1. The other substituents are Mg and Fe^{2+} in octahedral sites and Si in tetrahedral sites. The principal features of the cation ordering patterns are the same for all three samples:

1. Octahedral sites M1, M2, M7–M9 are Al rich; M4–M6 are Mg rich; and M3 is intermediate.

2. Si is strongly partitioned into T2. There is some disagreement about the location of the remaining Si. This is not surprising in view of the small quantity of Si involved, the similar scattering factors for Si and Al, and the strong degree of pseudosymmetry shown by the structure.

Table 1. (Al + Fe^{3+}) occupancies* in the cation sites of sapphirine

Site	PM	HR	SM	Site	PM	HR	SM
M1	1.00	0.96	1.00	T1	1.00	0.92	1.00
M2	1.00	0.94	1.00	T2	0.25	0.01	0.25
M3	0.50	0.44	0.25	T3	0.50	0.51	0.50
M4	0.00	0.00	0.00	T4	0.75	0.92	0.75
M5	0.00	0.00	0.00	T5	1.00	1.00	1.00
M6	0.00	0.00	0.00	T6	1.00	0.73	0.75
M7	1.00	1.00	1.00				
M8/9**	1.00	0.88	1.00				
Σ (Al + Fe)	4.50	4.22	4.25		4.50	4.09	4.25

Note: References are PM, Moore (1969); HR, Higgins and Ribbe (1979); SM, Merlino (1980).

* Remaining cations are (Mg + Fe^{2+}) in octahedral M sites, Si in tetrahedral T sites.

** M8 and M9 are not symmetrically distinct in the *2M* polytype.

This complex cation ordering scheme was rationalized by Moore (1969) as a compromise between the requirements of local charge balance and the minimization of electrostatic repulsion between cations.

The large variety of tetrahedral environments in sapphirine is of great interest from the point of view of NMR spectroscopy. The six symmetrically distinct tetrahedral sites are connected in open-branched vierer chains (Liebau, 1978). The sites along one of these chains are labeled as shown in Figure 1. T5 and T6 each have only one bridging O atom to other tetrahedra (Q^1 sites). T1 and T4 have two (Q^2), whereas T2 and T3 have three (Q_3). Si only comprises 20–33% of the tetrahedral cations in published sapphirine analyses, with the exception of an anomalous beryllian specimen (Deer et al. 1978; Higgins et al. 1979; Grew, 1981; Warren and Hensen, 1987; Christy, 1988b, 1989). Sapphirine must therefore contain a considerable number of tetrahedral Al-O-Al linkages, violating the "aluminum avoidance principle" attributed to Loewenstein (1954) and often invoked in the study of layer and framework silicates.

Thermodynamic properties

Kiseleva (1976) collated the experimental data of Chatterjee and Schreyer (1972), Newton (1972), Navrotsky et al. (1973), Newton et al. (1974), Doroshev and Malinovskiy (1974), and Kiseleva and Topor (1975) to derive thermodynamic data applicable to natural and synthetic sapphirine. Several assumptions were made about the stoichiometry and polytypic state of the sapphirine samples, but the calculated differences between thermodynamic quantities for the natural and synthetic materials appeared to be significant. Enthalpies of formation and entropies per mole of the 20–O atom formula unit are

natural sapphirine:

$$\Delta H^{f}_{298K,elmts} = -11114 \pm 8 \text{ kJ/mol}$$

$$S_{298K} = 382.3 \pm 1.7 \text{ J/mol·K}$$

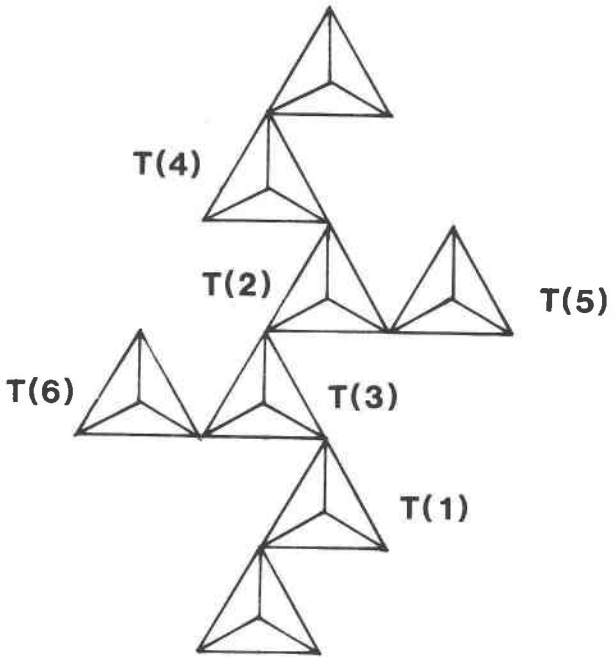

Fig. 1. The branched tetrahedral chain of sapphirine.

synthetic sapphirine:

$$\Delta H^{f}_{298K,elmts} = -11013 \pm 33.5 \text{ kJ/mol}$$

$$S_{298K} = 412.0 \text{ J/mol·K}.$$

Thus, the synthetic material is more endothermic by 101 kJ/mol and has a higher entropy by 29.7 J/mol·K.

If this entropy difference calculated by Kiseleva was purely configurational in origin, then it would correspond to around 60% disorder over all the cation sites. For a given cation distribution, the configurational entropy is $-R \Sigma n_i x_{i,j} \ln(x_{i,j})$. R is the gas constant (8.314 kJ/mol), n_i is the number of sites of type i in the formula unit, and $x_{i,j}$ is the proportion of site i occupied by atomic species j. Assuming that Mg, Al, and Si are long-range ordered as determined by the structure refinements, then the entropy increase due to disorder of Mg and Al in the octahedral sites and of Al and Si in the tetrahedral sites would be around 50 J/mol·K.

Experimental work

Sources, synthesis, and analysis of sapphirine for NMR study

The sapphirine samples examined using NMR in this study include synthetic samples with different compositions, synthesis conditions, and subsequent thermal histories, plus one natural sample. The presence of paramagnetic centers in the natural sample causes appreciable NMR line broadening (Oldfield et al., 1983). Thus, most of the NMR work concerns the Fe-free synthetic samples.

The synthetic samples were crystallized from gels in a piston-cylinder apparatus as described in Christy (1988a) and Christy and Putnis (1988). Several synthesis experiments under similar conditions (Table 2) were required to produce enough material for ^{29}Si NMR spectroscopy ($\simeq$300 mg). All products were heated in air at 850 °C to remove C and were further purified by flotation separation.

Table 2. Synthesis conditions and subsequent heat treatments for samples 1–5 of this study

Sample no.	$MgO:Al_2O_3:SiO_2$ of starting gel	Crystallization conditions*	Subsequent treatment
1	7:9:3	5 kbar, 1200 °C	—
2	7:9:3	5 kbar, 1200 °C	1 bar, 950 °C, 6 d
3	7:9:3	15 kbar, 1200 °C	—
4	7:9:3	15 kbar, 1200 °C	1 bar, 1200 °C, 6 d**
5	8:8:4	15 kbar, 1200 °C	—

* All crystallization experiments were 5 h in duration.
** Sample 4 initially held at 700 °C for 6 d. No change was observed in its NMR spectrum, so it was subsequently annealed at this higher temperature.

Microprobe analyses of the synthetic samples indicate that there is some compositional heterogeneity. The sapphirine Mg : Al : Si ratios do not necessarily correspond to those of the parent gels. Probe operating conditions are given by Christy (1989), where samples 1, 3, and 5 of this study are numbered 26, 27, and 29, respectively. Averages of the best analyses of that study (cation totals 13.90–14.10) are given in Table 3. Chemical heterogeneity was also indicated by X-ray powder diffraction (see below).

To test the hypothesis that the observed spectral differences between samples correspond to differences in the state of cation order, additional samples were prepared from a large batch of gel of the composition $7MgO \cdot 9Al_2O_3 \cdot 3SiO_2$. All products of experiments conducted under the same conditions were ground together and then purified by flotation separation. Samples of approximately 300 mg were then annealed in a muffle furnace at 950 °C for 14 d and at 1200 °C for 14 d. The samples were then reground and traces of Pt foil removed by hand picking. Their heats of solution were then determined in a Calvet twin-type solution calorimeter using $Pb_2B_2O_5$ flux at 970 K. The mean heats of solution from four successful experiments with each batch are reported below.

The natural sapphirine is from Aileron, central Australia, and has been described by Warren and Hensen (1987). The published analyses of this sapphirine show less than 2 wt% FeO, the lowest Fe content of any natural sapphirine of which we are aware. Attempts to obtain a spectrum from Mautia Hill sapphirine (4.4 wt% FeO; McKie, 1963; Christy, 1989) were unsuccessful. Both these sapphirine samples were examined using FTIR spectroscopy during the course of this study. Analytical data are presented in Table 3.

NMR spectroscopy

The spectrometers used for this study are similar to those described by Smith et al. (1983). The ^{29}Si MAS

TABLE 3. Microprobe analyses for synthetic and natural sapphirine samples

	Sample no.							
	1	3	5	6	7	8	9	10
SiO_2	13.04	13.15	16.74	11.00	12.15	14.28	14.57	16.13
Al_2O_3	63.63	62.72	57.63	69.00	67.20	61.61	57.93	58.94
FeO	—	—	—	0.53	4.65	7.30	4.44	3.93
MnO	—	—	—	—	—	—	0.24	—
MgO	20.00	20.23	22.42	19.12	16.94	18.73	21.28	20.53
CaO	—	—	—	—	—	—	—	0.16
Wt% total	96.69	96.10	96.79	99.65	100.94	100.97	98.46	99.79
	Cations per 20 O atoms							
Si	1.57	1.57	1.98	1.27	1.41	1.67	1.72	1.88
$^{[4]}Al$	4.43	4.43	4.02	4.68	4.59	4.20	3.84	4.02
Fe^{3+}	—	—	—	0.05	—	0.13	0.44	0.10
$^{[6]}Al$	4.47	4.40	4.03	4.71	4.61	4.31	4.23	4.12
Mg	3.54	3.60	3.97	3.29	2.93	3.10	3.75	3.57
Fe^{2+}	—	—	—	—	0.45	0.59	—	0.29
Mn	—	—	—	—	—	—	0.02	—
Ca	—	—	—	—	—	—	—	0.02
Total	14.01	14.00	14.00	14.00	13.99	14.00	14.00	14.00

Note: Sample provenance: 1 = synthetic, no. 26 of Christy (1989); 3 = synthetic, no. 27 (loc. cit.); 5 = synthetic, no. 29 (loc. cit.); 6 = Aileron, Australia (Warren and Hensen, 1987); 7 = Panrimalai, India, no. 13 of Christy (1989); 8 = Val Codera, Italy (no. 5, loc. cit.); 9 = Mautia Hill, Tanzania (no. 14, loc. cit.); 10 = Finero, Italy (no. 6, loc. cit.). Data for all analyses are means of data from 3 to 7 points.

NMR spectra of all the samples except no. 5 were obtained at $H_0 = 8.45$ T with spinning frequencies of 3.8–4.3 kHz. The spectrum of sample 5 was obtained at $H_0 = 11.7$ T. All pulse widths correspond to $\pi/4$ flip angles, varying from 6 to 4 μs. The recycle delay was 30 s for all ^{29}Si spectra except for that of the Aileron sample, which was obtained with a recycle delay of 5 s because of the small sample size and correspondingly weak signal. No significant change in the relative peak areas of the 7:9:3 samples was observed as the recycle delay was varied from 5 to 60 s. However, spectra obtained with shorter recycle delays had broader and more Lorentzian peaks, presumably due to an increased proportion of signal intensity from Si atoms near paramagnetic centers, which relax faster. The τ_1 of the 7:9:3 samples was about 2 s, whereas the τ_1 of the more siliceous 8:8:4 samples was about 20 s. The ^{27}Al spectra were obtained at $H_0 = 11.7$ T and a spinning frequency of 4.9 kHz. A pulse of 1 μs was used, where the nonselective $\pi/2$ pulse length was 9 μs. The recycle delay of 5 s corresponds to nearly complete relaxation of the ^{27}Al central transition resonance ($I = \frac{1}{2} \rightleftharpoons -\frac{1}{2}$).

Samples studied by infrared spectroscopy

Sources of the five natural sapphirine samples that were examined by FTIR, including the Aileron sample, are listed in the footnote to Table 3, which gives their microprobe analyses. The microprobe data are means of the analyses in Christy (1989), except for the analysis of the Aileron specimen. This is the most aluminous sapphirine described to date, sample 78921235B in Warren and Hensen (1987). The analysis given here is the mean of seven in that paper, with Fe^{3+} calculated by the method of Higgins et al. (1979).

An infrared spectrum was also obtained for a synthetic sapphirine sample, no. 1 of this study, and for the Panrimalai material after heating in a dry furnace at 1200 °C for 14 d.

Infrared spectroscopy

All samples were crushed to 70-mesh particle size and purified by flotation. The powders were then pressed into pellets with KBr. A Bruker 113v FTIR spectrometer was used for data measurement. Specimen preparation and experimental setup are as outlined in Güttler et al. (1989). Only room-temperature measurements were carried out since it was suspected that much of the observed peak overlap was due to the large number of infrared-active vibrations. Hence, resolution would not be improved at lower temperature.

RESULTS

NMR spectroscopy

The ^{27}Al NMR spectrum for synthetic sample 1 shows two resonances plus spinning sidebands (Fig. 2). The two true resonances have a 1:1 intensity ratio, corresponding to equal amounts of Al in fourfold and sixfold coordination (Kirkpatrick et al., 1985). This is consistent with the known crystal chemical relations of sapphirine (Moore, 1969).

Spectral features for Al in different sites of the same coordination number were not resolved at the magnetic field strength used. Therefore, ^{27}Al NMR study of the sapphirine was not pursued further.

The ^{29}Si NMR spectra of the synthetic samples contain four peaks, approximately evenly spaced, at about −73.1, −75.5, −78.0, and −80.0 ppm (Fig. 3). The positions of the peaks are nearly constant from sample to sample, but the relative intensities vary.

The overall spectral envelope of the Aileron sample (Fig. 4) is similar to those observed for the synthetic sam-

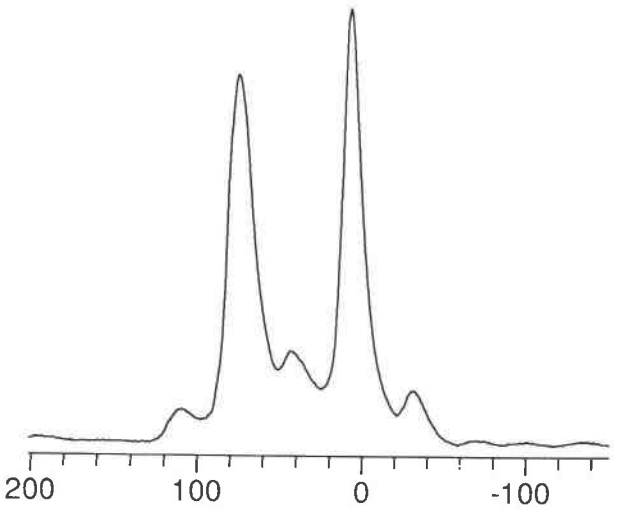

Fig. 2. The ^{27}Al NMR spectrum for synthetic sapphirine. The two largest peaks are real maxima; the smaller ones are spinning side bands.

ples. However, the Aileron spectrum is less well resolved, probably because of paramagnetic line broadening. For this sample, the strongest resonance occurs near −73 ppm, with a shoulder at −77 ppm and a broader resonance extending to beyond −80 ppm. It is probable that Si is distributed among the different tetrahedral environments in this sapphirine sample in much the same fashion as in the synthetic materials.

The ^{29}Si NMR spectrum for synthetic sample 5 was satisfactorily fitted with four Gaussian functions (Fig. 3, Table 4). These are labeled peaks 1–4 in order of increasing shielding. The spectra from samples 1–4 have higher signal/noise ratios. For these samples, the resonance near −78 ppm is clearly broad and non-Gaussian but was fitted as two overlapping Gaussian curves. The simulated peak areas for these are added to represent one region of intensity in later discussion.

The pressure of synthesis had little effect on relative peak areas (compare the spectra for samples 1 and 3). However, annealing at 950 °C and 1 bar for two weeks led to an increase in peak 2 intensity at the expense of peak 1 (sample 2). Annealing for 2 weeks at 1200 °C increased peak 2 intensity to an even greater degree (sample 4). For the silica-rich sample 5, peaks 2 and 3 are larger relative to peak 1 than for any of samples 1–4.

Calorimetry and X-ray diffraction of synthetic sapphirine

Heats of solution were measured for two samples that were heat treated identically to NMR samples 2 and 4. The mean values are 58.96 ± 1.01 kcal/mol for the sample annealed at 950 °C and 56.36 ± 0.38 kcal/mol for the sample at 1200 °C. The higher temperature material is therefore more endothermic by 2.60 ± 1.08 kcal/mol (10.9 ± 4.5 kJ/mol). This result suggests that cation disorder increases with annealing temperature. Thus, the reduction in intensity of peak 1 and increase in intensity of peak 2 in the ^{29}Si NMR spectrum for sample 4 are likely to be a consequence of increased Al-Si disorder.

Guinier powder X-ray diffraction photographs of the two samples used for calorimetry gave rise to no appre-

TABLE 4. Parameters for Gaussian peak fits to spectra of Figure 3

	Sample				
Peak	1	2	3	4	5
Peak 1					
I	0.484	0.459	0.485	0.412	0.356
δ	−73.223	−73.338	−73.038	−73.096	−72.940
w	1.350	1.380	1.313	1.506	1.543
Peak 2					
I	0.293	0.302	0.296	0.349	0.330
δ	−75.559	−75.648	−75.445	−75.456	−75.358
w	1.872	1.947	1.910	2.360	1.964
Peak 3a					
I	0.062	0.095	0.037	0.043	
δ	−77.609	−77.766	−77.400	−77.510	
w	1.111	1.315	0.839	1.067	
Peak 3b					
I	0.146	0.122	0.159	0.161	
δ	−78.677	−78.921	−78.494	−78.459	
w	1.643	1.378	1.661	1.802	
(3a + 3b)					
I	0.208	0.217	0.196	0.204	0.284
δ					−77.966
w					2.155
Peak 4					
I	0.014	0.021	0.025	0.035	0.031
δ	−81.000	−81.000	−80.666	−80.425	−81.000
w	1.943	2.108	1.348	2.158	1.476
1000 χ^2	0.1966	0.3735	0.4008	0.3314	0.1847
1000 × fract. sd	16.14	9.705	7.941	7.709	30.91

Note: *I* = relative peak area, δ = chemical shift, *w* = width of peak.

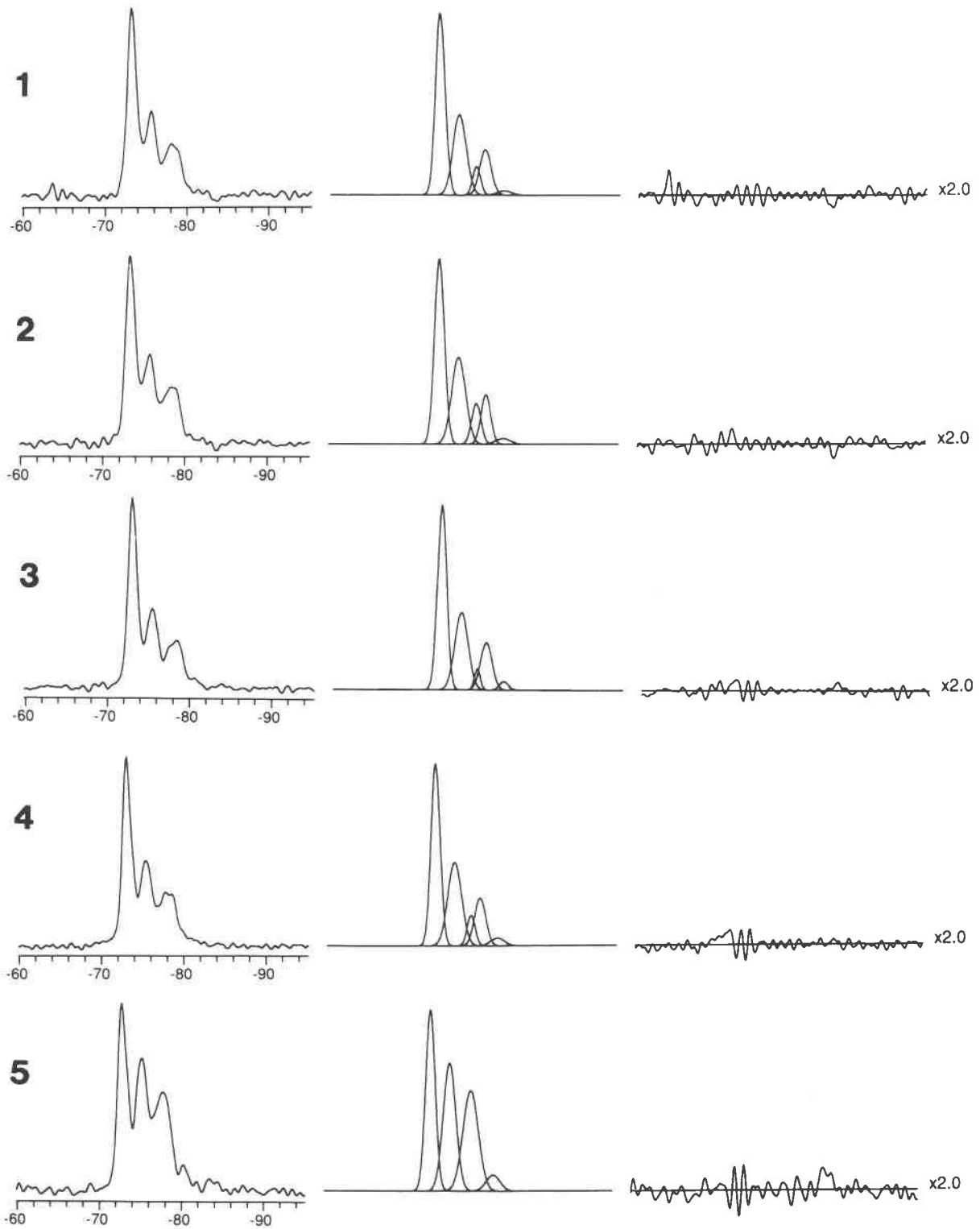

Fig. 3. The ^{29}Si NMR spectra and simulations for the synthetic sapphirine samples of this study. **(left)** Observed line envelopes. **(center)** Individual Gaussian curves comprising fitted envelopes. **(right)** Difference between observed and fitted spectra.

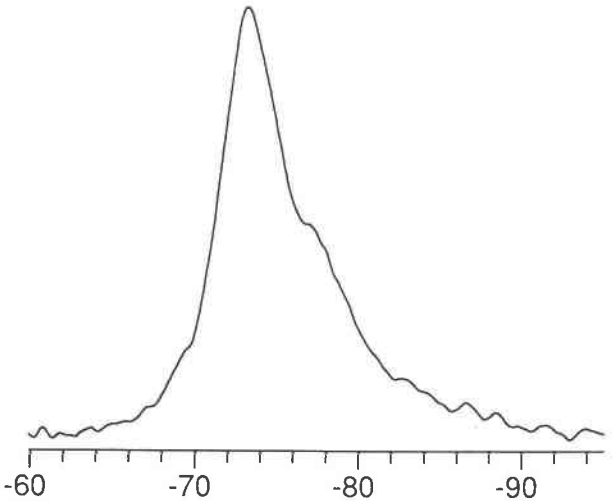

Fig. 4. The ^{29}Si NMR spectrum for the natural Aileron sapphirine sample.

ciable differences in lattice parameters. However, the stronger lines in both photographs are very broad. This broadening probably reflects chemical heterogeneity in the samples. Any change in cell parameters is obscured by the line broadening.

Infrared spectroscopy

All the spectra obtained are similar in their overall envelope (Fig. 5). However, a consistent loss of resolution with increasing Si content is apparent. This trend is not affected by the varying amounts of Fe and other minor constituents in the natural samples (analyses, Table 3). Figure 6a compares spectra from the Panrimalai sample before and after annealing at 1200 °C for 14 d. Figure 6b compares the spectrum of the synthetic sample 1 with that of Val Codera sapphirine, which has a similar Si content. The heat-treated and synthetic sapphirine samples show considerably less fine detail in their infrared spectra than their natural counterparts.

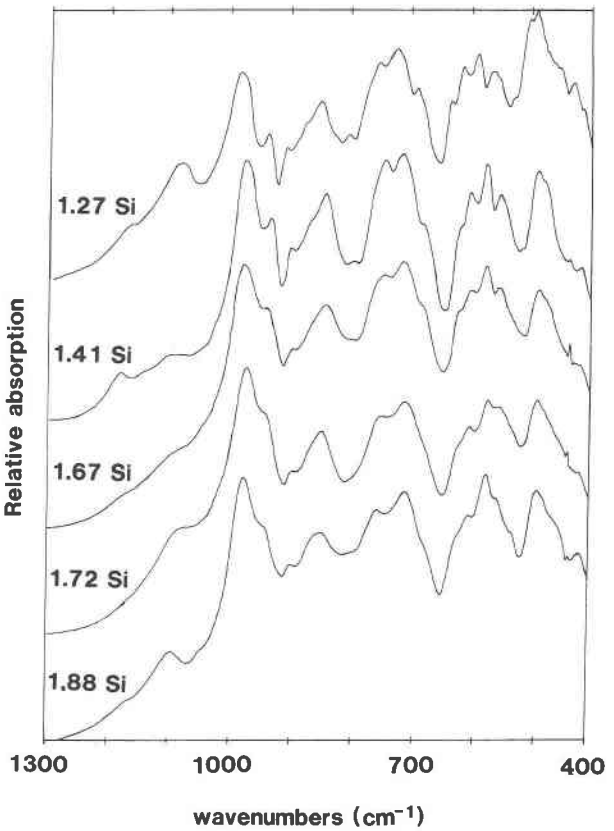

Fig. 5. IR spectra for natural samples 6–10, arranged in order of increasing Si content.

Interpretation of NMR spectra

Simulations

Assignment of the ^{29}Si MAS NMR peaks of sapphirine was difficult because of the large number of possible magnetically distinct Si sites in the sapphirine structure and the likely overlap of spectral intensity for different sites. Our assignment is based on computer simulations using the known structure of sapphirine and the known inverse correlation between Si shielding and the number of tetrahedral Al next-nearest neighbors (NNNs; cf. Kirkpatrick et al., 1985). The empirical correlations of Smith et al. (1983) and Sherriff and Grundy (1988) do not work well in this instance because the bond angles and distances derived for a given tetrahedral site are averages of the values for Al and Si on that site.

In making the assignments, we always assumed that for an Si atom in a given polymerization, Q^n, there were $(n + 1)$ possible peaks corresponding to $0,1 \ldots n$ tetrahedral Al NNNs and that shielding decreased as Si NNNs were replaced by Al. In addition, we assumed for some models that a $Q^n(x\text{Al})$ peak was more shielded than a $Q^m(x\text{Al})$ peak if $n > m$. However, this does not appear to be true for sapphirine.

The sapphirine ^{29}Si NMR spectral maxima, peaks 1–4, are near -73.1, -75.5, -78.0, and -80.0 ppm, respectively. Peak 1 is narrow and nearly Gaussian, which suggests that it may be due to just one type of local Si environment. Peak 2 is somewhat broader but may again be due to predominantly one type of Si environment. Peaks 3 and 4 are successively broader and are likely to be superpositions of unresolved contributions from Si in more than one type of environment (Fig. 3). The separation of the four main spectral maxima is 2.4–2.8 ppm, which we ascribe to Al-Si substitution on NNN sites, although such substitution usually causes a slightly larger change in chemical shift on Q^2 and Q^3 sites (3.5–4.2 ppm per NNN atom in $CaAl_2SiO_6$, 3.3–3.4 ppm in prehnite, 3.1 ppm in tremolite; B. L. Phillips, unpublished data). This small chemical shift change for sapphirine is probably due to its unusually small T-O-T angles (116–120°),

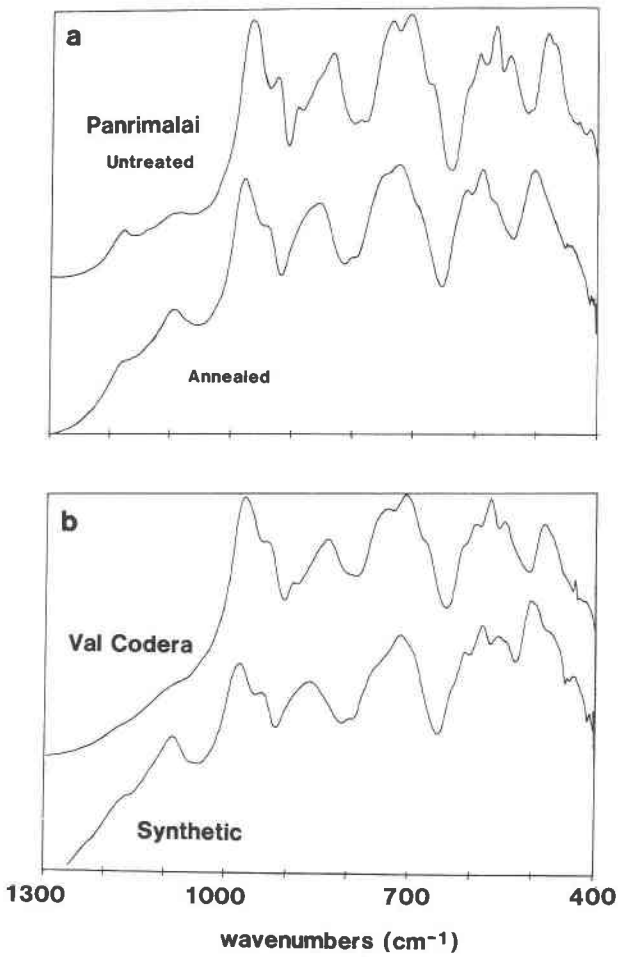

Fig. 6. (a) Spectra for sample 7 before 14 days' annealing at 1200 °C (above) and after annealing (below). (b) Comparison of spectra of synthetic sample 1 and natural sample 8, which have similar Si contents.

which are a consequence of the O close packing and strong bonding of bridging O atoms to octahedral Mg in this structure. Only the 115° Si-O-Al bond angle in sillimanite is known to be smaller (Burnham, 1963; Higgins and Ribbe, 1979).

The structure refinements indicate that most of the Si in sapphirine should be in Q^3 (3 Al) and Q^3 (2 Al) environments. Thus, it is reasonable to assign the largest peak (peak 1, at −73 ppm) to Q^3 (3 Al). This assignment is supported by the observed ^{29}Si NMR resonance at −73 ppm for margarite, which has all of its Si in Q^3 (3 Al) sites and T-O-T bond angles of only 121° (Guggenheim and Bailey, 1975; Sanz and Serratosa, 1984). However, it should be noted that the Q^3 (3 Al) Si of sillimanite is much more shielded ($\delta = -87$ ppm; Smith et al., 1983).

In order to determine the combinations of peak assignments and Al-Si ordering patterns that were consistent with the NMR data, we first tried the peak assignment models numbered 1–5 in Table 5. For each assignment scheme, the calculated intensities for the four peaks were

TABLE 5. Peak assignment schemes for Si-Al distribution models used to fit the ^{29}Si NMR spectra of this study

Model no.	Peak 1 −73 ppm	Peak 2 −75.5	Peak 3 −78	Peak 4 −80.5
1	Q^1(1 Al)	Q^1(0 Al)		
	Q^2(2 Al)	Q^2(1 Al)	Q^2(0 Al)	
	Q^3(3 Al)	Q^3(2 Al)	Q^3(1 Al)	Q^3(0 Al)
2	Q^1(1 Al)	Q^1(0 Al)		
	Q^2(2 Al)	Q^2(1 Al)	Q^2(0 Al)	
		Q^3(3 Al)	Q^3(2 Al)	Q^3(1 Al)
3	Q^1(1 Al)	Q^1(0 Al)		
		Q^2(2 Al)	Q^2(1 Al)	Q^2(0 Al)
		Q^3(3 Al)	Q^3(2 Al)	Q^3(1 Al)
4	Q^1(1 Al)	Q^1(0 Al)		
		Q^2(2 Al)	Q^2(1 Al)	Q^2(0 Al)
			Q^3(3 Al)	Q^3(2 Al)
5	Q^1(1 Al)	Q^1(0 Al)		
	Q^2(2 Al)	Q^2(1 Al)	Q^2(0 Al)	
			Q^3(3 Al)	Q^3(2 Al)
6		Q^1(1 Al)	Q^1(0 Al)	
		Q^2(2 Al)	Q^2(1 Al)	Q^2(0 Al)
	Q^3(3 Al)	Q^3(2 Al)	Q^3(1 Al)	Q^3(0 Al)
7			Q^1(1 Al)	Q^1(0 Al)
		Q^2(2 Al)	Q^2(1 Al)	Q^2(0 Al)
	Q^3(3 Al)	Q^3(2 Al)	Q^3(1 Al)	Q^3(0 Al)

followed as the Si contents of the tetrahedral sites were varied. Some of the models assigned peak 1 to Q^3 (3 Al); others did not.

Models 1–5 assumed that Si enters both sites of a given Q state equally and constrained the total Si content to be 1.95 per formula unit. No Al-Si distributions gave a good fit to the observed peak intensities for models 1 or 5. However, simulations using models 2–4 showed two general ordering patterns that fit the observed data to within three standard deviations: (1) Models 2 and 3: 0.66 Si in each Q^1 site, most of the remainder in Q^3. (2) Models 3 and 4: 0.51–0.52 Si in each Q^1 site, most of the rest in Q^2.

Simulations were also calculated in which the average Si occupancies were not constrained to be equal for sites of the same Q state and in which short-range order was permitted. However, fits for models 2–4 were only slightly improved by changing these constraints.

The successful ordering patterns for models 1–5 were clearly questionable. Si was preferentially placed on the least-polymerized tetrahedral sites, whereas the structure refinements suggest placement of Si on the Q^3 sites, in accord with crystal chemical principles. Therefore, we rejected models 1–5.

Much better fits were obtained if the strong, narrow peak at −73 ppm was attributed to Q^3 (3 Al) only, as in models 6 and 7 (Table 5). These assignment schemes are unusual in that they assume that polymerization state has little effect on ^{29}Si chemical shift for a given number of Al NNNs. Fitting for these assignment schemes was performed as follows:

1. Si_{tot} was taken to be either 1.5 (the 7:9:3 composition, close to that of samples 1–4) or 1.8 (more relevant to sample 5).

2. The Si was initially distributed uniformly over all

TABLE 6. Numbers of Si-O-Si, Si-O-Al, and Al-O-Al linkages for various Al-Si distributions in sapphirine

LRO scheme	1	2	3	4	5	6
T1	0.25	0.125	0.00	0.318	0.08	0.08
T2	0.25	0.625	0.75	0.318	0.74	0.99
T3	0.25	0.625	0.50	0.318	0.74	0.49
T4	0.25	0.125	0.25	0.318	0.08	0.08
T5	0.25	0.000	0.00	0.318	0.135	0.00
T6	0.25	0.000	0.00	0.318	0.135	0.27
Σ Si	1.50	1.50	1.50	1.91	1.91	1.91
No. of						
SiOSi	0.375	0.563	0.563	0.607	0.872	0.742
SiOAl	2.225	3.125	3.125	2.602	3.286	3.546
AlOAl	3.375	2.313	2.313	2.791	1.842	1.712
(no additional SRO)						
SiOSi	0.00	0.25	0.25	0.00	0.48	0.55
SiOAl	3.00	3.75	3.75	3.816	4.07	3.93
AlOAl	3.00	2.00	2.00	2.184	1.45	1.52
(maximum SRO)						

Note: Ordering patterns 1–3 are for the stoichiometry of Moore (1969), schemes 4–6 for the higher Si content of Higgins and Ribbe (1979). Schemes 1 and 4 show complete long-range disorder of (Si,Al). Schemes 2 and 5 apportion Si equally between both sites of a given degree of polymerization. Schemes 3 and 6 correspond to the structure refinements. Making the LRO occupation pattern more asymmetrical and introducing short-range order both increase the number of Si-O-Al links appreciably.

six sites, and peak areas were calculated assuming no short-range Al-Si order.

3. The calculation was repeated after trial exchanges of Si and Al between sites. Exchanges giving an improvement in overall fit were retained for the next iteration.

Table 6 lists the Si distributions that gave the best fits.

Only the spectrum for sample 5 was well fitted in simulations with $Si_{tot} = 1.8$. A strong positive correlation between the areas of peaks 1–3 precluded this composition fitting the spectra for the more aluminous samples. Conversely, calculations assuming $Si_{tot} = 1.5$ successfully fitted samples 1–4 but not sample 5.

An important feature of all the successful simulations with models 6 and 7 was that peaks 1 and 2 could only be fitted satisfactorily if one Q^3 site was almost fully occupied by Si and the other was much less so. This asymmetrical occupancy is due to the assignment of peak 1 to Q^3 (3 Al). Since the two Q^3 sites are adjacent, appreciable concentrations of Si on both sites would lead to the formation of Si-O-Si linkages. Q^3 (2 Al) intensity would then be developed at the expense of the Q^3 (3 Al) peak. Although the simulations did not distinguish T2 from T3, this result is qualitatively consistent with the ordering schemes derived from diffraction data, in which T2 is more Si rich than T3.

The simulations imposed little constraint on the occupancies of the Q^1 and Q^2 sites. The amount of Si in these sites was small for all successful simulations. Therefore, cation exchange among them had little effect on the calculated relative peak areas.

Other encouraging features of models 6 and 7 are listed below:

1. The spectrum of the siliceous sample 5 was fitted better when the Si total in the simulation was larger.

2. Sample 4, held at 1200 °C for 2 weeks, gave a spectrum which was fitted best when some Si was left disordered over all the sites. This observation is consistent with the more positive enthalpy for this sample than for sample 2 determined by calorimetry.

3. The number of overlapping resonances corresponding to different Si environments increases with increasing shielding for these models, in accord with the progressive broadening of the observed peaks.

Short-range vs. long-range order

The best simulations in this study appear to be those in which one Q^3 site is almost fully occupied by Si and the other site is virtually pure Al. The difference between the two Q^3 sites is much greater than that implied by the single-crystal diffraction studies, which put significant Si into both T2 and T3. This discrepancy suggests that these sites may display considerable short-range order (SRO), which cannot be detected by X-ray or neutron diffraction. SRO data are averaged out as a consequence of the large correlation length ($\simeq$100 Å) for these techniques compared with NMR.

The Al-Si ordering schemes considered in the simulations were all long-range ordering (LRO) patterns. For most simulations, no additional short-range preference was considered for Si-O-Al over Si-O-Si or Al-O-Al linkages. The assumption of no SRO allowed straightforward comparison of our deduced Si occupation patterns with those of the structure refinements. However, the LRO behavior is likely to be an average of several SRO configurations. Unlike diffraction techniques, NMR does provide information about immediate nearest-neighbor and NNN environments. Our simulations suggest that Si enters only one of T2 or T3 per asymmetric unit in sapphirine. The structure determinations indicate an LRO scheme with 0.75–1.00 Si in T2 and ~0.5 Si in T3. These observations are reconciled if the LRO pattern is an average of two SRO schemes. We propose that in the majority of asymmetric units in the structure, T2 is Si and T3 is Al. In some cases (30–40%), the converse is true.

Occupation of both Q^3 sites by Si would imply the existence of an Si-O-Si link between the sites. Avoidance of such a situation is readily understood on reconsideration of Loewenstein's Al avoidance principle. The thermodynamic rationale for Al avoidance is the highly endothermic nature of the exchange reaction 2[Al-O-Si] → [Al-O-Al] + [Si-O-Si]. The enthalpy for this reaction is +34 kJ/mol in cordierite (Putnis, 1988). A value of +25.8 kJ/mol may be calculated for the corresponding reaction in albite from the data of Carpenter et al. (1985). The albite figure is clearly comparable in magnitude to that for cordierite, despite the much smaller Al/Si ratio of albite.

Table 6 shows the number of Si-O-Si, Si-O-Al, and Al-O-Al linkages per asymmetric unit for various LRO patterns in sapphirine. The proportion of Si-O-Al linkages is much higher if Si is concentrated into Q^3 sites than if Si is randomly distributed or is preferentially in Q^1 sites.

The number of Si-O-Al links is increased further if the two Q^3 sites have unequal Si occupancies. Therefore, the LRO and SRO patterns of Si occupancy implied by the diffraction and NMR data maximize the number of Si-O-Al linkages and presumably reduce the enthalpy of the structure considerably. Nevertheless, the tetrahedral Al/Si ratio in sapphirine is too high to avoid Al-O-Al linkages completely.

Good fits to the ^{29}Si NMR spectra were obtained using models that took SRO into account. In this simulation, the two sites of a given Q^n state were not differentiated, but a short-range order parameter P was incorporated. The value $P = 1$ maximized the number of Al-O-Si bonds for a given Si content in Q^1, Q^2, and Q^3 sites. $P = 0$ corresponded to no such preference. Si_{tot} was assumed to be 1.5 for samples 1–4 and 1.8 for sample 5. Assignment schemes 1, 4, and 7 were tried with this model. Scheme 1 did not give good fits, whereas schemes 4 and 7 fit satisfactorily. However, only assignment scheme 7 had Si in Q^3 preferentially, consistently gave the best fits with high values of P, and hence allowed a high proportion of Si-O-Al linkages.

Thus, it appears that assignment scheme 7, with Si preferentially on Q^3 sites and considerable short-range order maximizing the proportion of Si-O-Al linkages, provides the best interpretation of the ^{29}Si NMR spectrum of sapphirine. The Si site occupancies and SRO parameters that gave best fits to the data with assignment scheme 7 are shown in Table 7.

Discussion of FTIR spectra

Resolution of individual vibrational modes is not possible for sapphirine because of the large size and low symmetry of the unit cell. For instance, the *2M* polytype has 34 atoms in the asymmetric unit of its structure, all in the general position of multiplicity 4. Factor group analysis shows that $\Gamma_{cell} = 102\ A_g + 102\ B_g + 102\ A_u + 102\ B_u$. The acoustic modes are of species $A_u + 2B_u$, leaving a total of 201 infrared-active ungerade modes. Many of these are likely to correspond to internal bending and stretching modes within the wavenumber range of this study. Hence, the maxima in the absorption envelopes are probably superpositions of several modes. Therefore, no quantitative line-width or line-shape information can be obtained for these spectra. Nevertheless, it is noteworthy that progressively fewer distinct maxima and minima are seen in the envelopes as Si content increases (Fig. 5). The loss of resolution suggests that line width for the individual modes increases with Si content. This in turn implies that the diversity of Si environments increases on the scale of the infrared correlation length (~30 Å). Such behavior is consistent with the NMR spectroscopy and the cation ordering pattern deduced from it. One Si atom per formula unit appears to order into a Q^3 site. The remaining Si atom does not appear to have a strong site preference. Therefore, cation disorder increases with increasing Si.

Table 7. Best fits to data for Si-Al distribution model allowing variable tendency toward short-range order, using peak assignment scheme 7

	Sample				
	1	2	3	4	5
Calc. peak intensities					
1	0.473	0.460	0.491	0.419	0.357
2	0.286	0.306	0.305	0.352	0.329
3	0.212	0.217	0.193	0.210	0.281
4	0.013	0.018	0.012	0.018	0.032
$10^6(I_c - I_0)^2$*	91	26	295	383	12
Si content per site					
Q^1	0.155	0.154	0.130	0.130	0.239
Q^2	0.044	0.066	0.130	0.130	0.130
Q^3	0.551	0.531	0.490	0.490	0.531
SRO parameter	0.75	0.65	0.70	0.55	0.65
Number of linkages					
Si-O-Al	3.38	3.31	3.41	3.26	3.62
Si-O-Si	0.21	0.22	0.15	0.23	0.28
Al-O-Al	2.42	2.47	2.43	2.51	2.10

* I_0 are fitted peak intensities as presented in Table 4.

Conclusions

Our ^{29}Si NMR spectra indicate that the Si environments in natural sapphirine and synthetic sapphirine are similar. The spectrum from natural Aileron sapphirine is not well resolved, probably because of paramagnetic line broadening. The spectra from the Fe-free synthetic samples are resolved into discrete peaks, which we have assigned so as to place most of the Si into Q^3 sites, consistent with the published structure refinements for natural sapphirine.

In our simulations, the spectra are best fitted if one Q^3 site per asymmetric unit is completely occupied by Si but the neighboring Q^3 site is Si-free. This result implies the presence of considerable short-range order in sapphirine. This short-range order reduces the enthalpy of the structure by maximizing the number of Si-O-Al links in the tetrahedral chains. This is a modification of Loewenstein's "aluminum avoidance principle"; it is not possible to eliminate all the Al-O-Al links in sapphirine because the Al : Si ratio is too high.

The simulations do not constrain the location of the remaining Si in excess of 1 atom per formula unit. The NMR spectrum of a relatively siliceous synthetic sample (~1.8 Si per formula unit) suggests that both short-range and long-range order decrease as Si content increases. This conclusion is supported by infrared spectra of natural sapphirine, which show a loss of resolution with increasing Si that appears analogous to the spectral change observed on high-temperature annealing.

One can speculate that sapphirine with only one Si atom per 20 O atoms, $(Mg_3Al_5)(Al_5Si)O_{20}$, would be fully ordered. However, this composition—the 3:5:1 composition of Warren and Hensen (1987)—appears to be unstable with respect to spinel-bearing assemblages. In general, natural sapphirine has 1.2–2.0 Si per formula unit. It seems likely that the configurational entropy associated with Al-Si disorder on the Q^1 and Q^2 sites plays a role in stabilizing sapphirine. Short-range order in T2 and T3

does not detract appreciably from the total entropy available. The entropy associated with a random distribution of 1 Si over each T2 + T3 pair would be $2R \ln 2 = 11.5$ J/mol·K. If short-range order occurs so that one site out of each pair is occupied by Si, T2 70% of the time and T3 30% of the time, the associated entropy is $-R(0.7 \ln 0.7 + 0.3 \ln 0.3) = 5.1$ J/mol·K. The entropy reduction associated with short-range ordering for these sites is therefore an order of magnitude smaller than the configurational entropy available from disorder on the octahedral and remaining tetrahedral sites (~50 J/mol·K).

Sapphirine appears to be stabilized as a phase in the MgO-Al_2O_3-SiO_2 system through a combination of short-range order in T2 and T3 to maximize the number of tetrahedral Si-O-Al linkages, and disorder on the remaining tetrahedral sites.

Acknowledgments

We would like to thank R.G. Warren and B.J. Hensen for their kind provision of the Aileron sample and M.A. Carpenter for performing the calorimetry. A.G.C. was supported at the University of Cambridge during this work by a Ph.D. studentship from the Natural Environment Research Council of Great Britain. The study was also supported by NSF grant EAR-8706929 (R.J.K., B.L.P.).

The text of this paper was much improved after the comments of David L. Bish and two anonymous referees.

References cited

Burnham, C.W. (1963) Refinement of the crystal structure of sillimanite. Zeitschrift für Kristallographie, 118, 127–148.

Carpenter, M.A., McConnell, J.D.C., and Navrotsky, A. (1985) Enthalpies of ordering in plagioclase feldspar solid solutions. Geochimica et Cosmochimica Acta, 49, 947–966.

Chatterjee, N.D., and Schreyer, W. (1972) The reaction enstatite$_{ss}$ + sillimanite = sapphirine$_{ss}$ + quartz in the system MgO-Al_2O_3-SiO_2. Contributions to Mineralogy and Petrology, 36, 49–62.

Christy, A.G. (1988a) The structure and stability of sapphirine in relation to its metamorphic environment. Ph.D. thesis, University of Cambridge, Cambridge, England.

——— (1988b) A new 2c superstructure in beryllian sapphirine from Casey Bay, Enderby Land, Antarctica. American Mineralogist, 73, 1134–1137.

——— (1989) The effect of composition, pressure and temperature on the stability of the 1Tc and 2M polytypes of sapphirine. Contributions to Mineralogy and Petrology, 103, 211–225.

Christy, A.G., and Putnis, A. (1988) Planar and line defects in the sapphirine polytypes. Physics and Chemistry of Minerals, 15, 548–558.

Deer, W.A., Howie, R.A., and Zussmann, J. (1978) Rock-forming minerals, vol. 2A: Single-chain silicates. Longman, London.

Doroshev, A.M., and Malinovskiy, I.Yu. (1974) Verkhnyaya po daleniyu granitsa ustoichivosti sapfirina. Doklady Akademii Nauk SSSR, 219, 959–961.

Grew, E.S. (1981) Surinamite, taaffeite and beryllian sapphirine from a pegmatite in granulite-facies rocks in Casey Bay, Enderby Land, Antarctica. American Mineralogist, 66, 1022–1033.

Guggenheim, S., and Bailey, S.W. (1975) Refinement of the margarite structure in subgroup symmetry. American Mineralogist, 60, 1023–1029.

Güttler, B.K., Salje, E., and Putnis, A. (1989) Structural state of Mg-cordierite III: Infrared spectroscopy and the nature of the hexagonal-modulated transition. Physics and Chemistry of Minerals, 16, 365–373.

Hensen, B.J. (1987) P-T grids for undersaturated granulites in the systems MAS (n+4) and FMAS (n+3)—tools for the derivation of P-T paths of metamorphism. Journal of Metamorphic Geology, 5, 255–272.

Higgins, J.B., and Ribbe, P.H. (1979) Sapphirine II: A neutron and X-ray diffraction study of Mg-Al and Al-Si ordering in monoclinic sapphirine. Contributions to Mineralogy and Petrology, 68, 357–368.

Higgins, J.B., Ribbe, P.H., and Herd, R.K. (1979) Sapphirine I: Crystal chemical contributions. Contributions to Mineralogy and Petrology, 68, 349–356.

Kirkpatrick, R.J. (1988) MAS NMR spectroscopy of minerals and glasses. In Mineralogical Society of America Reviews in Mineralogy, 18, 341–404.

Kirkpatrick, R.J., Smith, K.A., Schramm, S., Turner, G., and Young, W.H. (1985) Solid state NMR spectroscopy of minerals. Annual Review of Earth and Planetary Sciences, 13, 29–47.

Kiseleva, I.A. (1976) Thermodynamic parameters of natural, ordered sapphirine and synthetic, disordered sapphirine. Geochemistry International, 13, 113–122.

Kiseleva, I.A., and Topor, N.D. (1975) Vysokotemperaturnaya teployemkost' sapfirina (high-temperature heat capacity of sapphirine). Geokhimiia, 1975, 312–315.

Liebau, F. (1978) Silicates with branched anions: A crystallochemically distinct class. American Mineralogist, 63, 918–923.

Loewenstein, W. (1954) The distribution of aluminum in the tetrahedra of silicates and aluminates. American Mineralogist, 39, 92–96.

McKie, D. (1963) Order-disorder in sapphirine. Mineralogical Magazine, 33, 635–645.

Merlino, S. (1973) Polymorphism in sapphirine. Contributions to Mineralogy and Petrology, 41, 23–29.

——— (1980) The crystal structure of sapphirine-1Tc. Zeitschrift für Kristallographie, 151, 91–100.

Moore, P.B. (1969) The crystal structure of sapphirine. American Mineralogist, 54, 31–49.

Navrotsky, A., Newton, R.C., and Kleppa, O.J. (1973) Sillimanite-disordering enthalpy by calorimetry. Geochimica et Cosmochimica Acta, 37, 2497–2508.

Newton, R.C. (1972) An experimental determination of the high-pressure stability limits of magnesium cordierite under wet and dry conditions. Journal of Geology, 80, 398–420.

Newton, R.C., Charlu, T., and Kleppa, O.J. (1974) A calorimetric investigation of the stability of anhydrous magnesium cordierite with application to granulite facies metamorphism. Contributions to Mineralogy and Petrology, 44, 295–311.

Oldfield, E., Kinsey, R.A., Smith, K.A., Nichols, J.A., and Kirkpatrick, R.J. (1983) High-resolution NMR of inorganic solids. The influence of magnetic centers on magic-angle sample-spinning lineshapes in some natural aluminosilicates. Journal of Magnetic Resonance, 51, 325–329.

Putnis, A. (1988) Solid-state NMR and phase transitions in minerals. In E.K.H. Salje, Ed., Phase transitions and thermodynamic properties of minerals. NATO ASI Series C, vol 225. Reidel, Dordrecht, the Netherlands.

Sahama, Th.G., Lehtinen, M., Rehtijärvi, P., and von Knorring, O. (1974) Properties of sapphirine. Annales Academiae Scientarum Fennicae A.III, 114, 1–23.

Sanz, J., and Serratosa, J.M. (1984) ^{29}Si and ^{27}Al high-resolution MAS NMR spectra of phyllosilicates. Journal of the American Chemical Society, 106, 4790–4793.

Schreyer, W., and Seifert, F. (1969) Compatibility relationships of the aluminium silicates in the systems MgO-Al_2O_3-SiO_2-H_2O and K_2O-MgO-Al_2O_3-SiO_2-H_2O at high pressure. American Journal of Science, 267, 371–388.

Sherriff, B.L., and Grundy, H.D. (1988) Calculation of ^{29}Si MAS NMR chemical shifts from silicate mineral structures. Nature, 332, 819–822.

Smith, K.A., Kirkpatrick, R.J., Oldfield, E., and Hudson, D.M. (1983) High resolution silicon-29 nuclear magnetic resonance spectroscopy of rock-forming silicates. American Mineralogist, 68, 1206–1215.

Strens, R.G.J. (1974) The common chain, ribbon and ring silicates. In V.C. Farmer, Ed., The infrared spectra of minerals. The Mineralogical Society of Great Britain, London.

Warren, R.G., and Hensen, B.J. (1987) Peraluminous sapphirine from the Aileron district, Arunta block, central Australia. Mineralogical Magazine, 51, 409–416.

Manuscript received April 6, 1990
Manuscript accepted August 31, 1991